

Dielectric Properties of the bR Membrane

Irina Ermolina, Aaron Lewis, and Yuri Feldman*

Department of Applied Physics, The Hebrew University of Jerusalem, Jerusalem 91904, Israel

Received: December 30, 2002; In Final Form: July 29, 2003

The application of dielectric spectroscopy (DS) to the study of bacteriorhodopsin (bR)-containing purple membrane films is presented in this paper. Two types of bR membrane films, oriented and nonoriented, were investigated in a wide frequency range (10^{-2} – 3×10^9 Hz) and temperature interval (5–70 °C). Four relaxation processes were observed in this frequency range and ascribed to different mechanisms, related to the structural units of the system. A large nonreversibility of the dielectric response as a result of heating and cooling has been observed in the slow processes implicating a change in the structure of the membrane stacking depending on the history of cooling and heating of the sample. Significant changes as large as 3 orders of magnitude in the mobility have been observed in this time scale. Comparison of the oriented and nonoriented bR membrane films was performed, and it was found that the oriented purple membrane has a unique liquid crystal-like ferroelectric behavior.

1. Introduction

Bacteriorhodopsin (bR) is an integral membrane protein that is found in the purple membrane of the bacterium *Halobacterium salinarum*. The purple membrane is a two-dimensional crystalline lattice formed by bacteriorhodopsin and lipid molecules in the cytoplasmic membrane of this bacterium. The function of bR in the purple membrane is that of a light driven proton pump.

The purple membrane of *Halobacterium halobium* consists of 25% of the lipid bilayer and 75% of bacteriorhodopsin protein, and therefore, this purple membrane is usually called bacteriorhodopsin membrane or shortly bR membrane. The function of this system is a light-driven proton pump, and the resulting electrochemical gradient is used by the cell to drive ATP synthesis and other metabolic processes under anaerobic conditions (flash excitation). The bR molecule, with the molecular weight of 25 kD, contains seven closely packed α -helices crossing the membrane (Figure 1a) and a Retinal group playing the keynote role in the function of this protein. Every α -helix has a ~ 50 D dipole moment and six of them compensate each other. bR molecules are packed in the membrane in very specific way. Every three macromolecules are placed close to each other in a certain position and form the triad (Figure 1b). It is known that these triads are maximally packed in a hexagonal way in the membrane.¹ The dipole moment of each macromolecule crosses the membrane in the same direction. A fragment of bR membrane is schematically presented in Figure 1b.

In the past 25 years since its discovery, numerous biophysical measurements have been performed on this important system in biological energy transduction.^{2,3} However, the fundamental mechanisms that underlie this molecular system still remain a major question in biophysics.

It is clear today that one of the key components in the function of this membrane protein is the movement of charge and the motion of dipolar groups in the membrane.³ A well-known methodology to investigate such movements in charged and

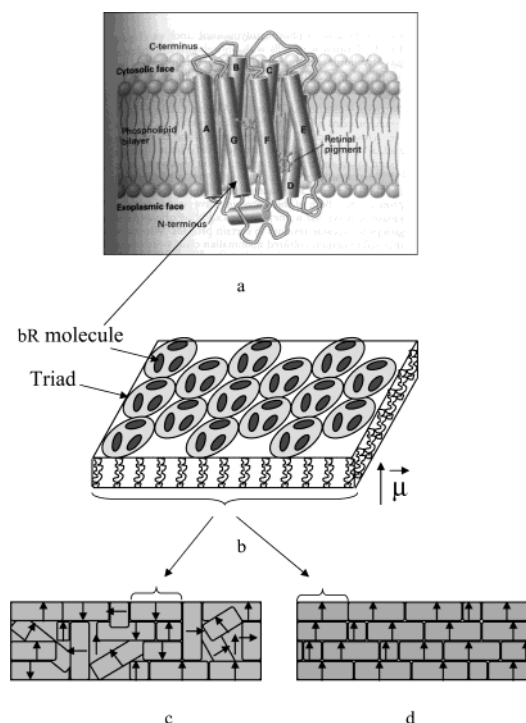


Figure 1. Schematic presentation of a single bR molecule in the membrane (a); package of bR molecules in the membrane fragment (b); and nonoriented (c) and oriented (d) bR membrane films.

polar groups is dielectric spectroscopy. The values of the permanent and induced electric dipoles, as well as the angle of the retinal to the membrane plane normal, depend on different parameters including membrane fragment size, distance between the membrane fragments, and the ionic environment. The permanent dipole moment, polarizability, and the retinal angle of *Halobacterium halobium* purple membranes were determined by Barabas et al.⁴ at different pH values. All of the parameters have a maximum between pH 5 and 6. There is a reversal in the direction of the permanent dipole moment near pH 5. The value of the permanent dipole moment was determined to be

* To whom correspondence should be addressed. E-mail: yurif@vms.huji.ac.il.

60 D/protein at pH 6.6, and the value obtained for polarizability was 3×10^{-28} Fm²/membrane fragment. The retinal angle of all-trans retinal was 0.8° smaller than that of the 13-cis conformations.

A purple membrane suspension shows two different orientations in electric fields of different frequencies. The orientation at low frequencies (≤ 10 Hz), with the membrane surface perpendicular to the electric field, is due to the permanent dipole moment of the membrane, and the orientation at high frequencies (≥ 100 Hz), with the surface parallel to the electric field, is due to the induced dipole moment (~ 500 kD to 10 MD and was proportional to the square of the diameter of the membrane). Using the membrane size from electron microscopy, a value of the dipole moment being equal to 98 D per one bacteriorhodopsin macromolecule was obtained. It was also concluded⁵ that the direction of the permanent dipole moment was from cytoplasmic to the extra-cellular side. These values, however, were strongly dependent on the ionic strength in the medium, suggesting a screening effect due to counterions near the membrane surface. The evaluation of the screening effect showed about a four-charge difference between the two sides of the purple membrane. It was shown that under illumination the permanent dipole moment decreased from 98 to 63 D/bacteriorhodopsin. These results were confirmed independently by linear and transient dichroism methods.⁶ Note that all of the mentioned results were obtained in the purple membrane suspension. The dielectric spectroscopy has not been applied to the comprehensive study of bR PM in the state of oriented and nonoriented films.

The main aim of this work is the application of time domain dielectric spectroscopy (TDDS) from 500 kHz to 3 GHz to the bR containing purple membrane film. The application of such a probe to the purple membrane not only has import for understanding the structure and the dynamics of this important biophysical system but also has broader implications for elucidating the forces and the structural dynamics that are responsible for the assembly and stability of integral membrane protein complexes. The wealth of data on the purple membrane should allow us to analyze our results in terms of the best models that define the structural basis of macromolecular complexes.

2. Materials and Methods

2.1. Preparation of the Membrane Films. In the current work, the two types of bR membrane films are studied. The type of the sample depends on the preparation. When the film is obtained by a simple drying, the fragments of bR membrane are packed randomly (Figure 1c) and such a film is called a nonoriented bR membrane film. The oriented sample is prepared by depositing purple membrane fragments on the electrode in an electric field (Figure 1d).

Purple membrane film was produced by procedure described by Varo.⁷ First, the base suspension of bR membrane fragments was stored up. With such membranes, two groups of samples were prepared: oriented and nonoriented films. The nonoriented film was obtained by simple drying of the suspension portion at the electrode surface. The oriented film was prepared by depositing purple membrane fragments on the electrode in an electric field.⁸ The thickness of the samples was varied from 20 up to 30 μ m. All samples were investigated using three dielectric spectrometers and a differential scanning Calorimeter in the temperature range from 5 up to 70 °C.

2.2. Dielectric Spectroscopy. The dielectric spectroscopy (DS) method occupies a special place among the numerous modern methods used for physical and chemical analysis of

material, because it enables investigation of dielectric relaxation processes in an extremely wide range of characteristic times (10^4 – 10^{-12} s). In this work, we applied two different dielectric spectrometers: (a) broad band dielectric spectrometer (BDS) and (b) time domain dielectric spectrometer (TDDS).

a. Broad Band Dielectric Spectrometer (BDS). Dielectric measurements in the frequency range of 10^2 – 10^7 Hz were performed using a Solartron-Schlumberger frequency response analyzer FRA 1260 with a Novocontrol active cell BDC–S. The sample temperatures were controlled by Novocontrol QUATRO Cryosystem.

b. Time Domain Dielectric Spectrometer (TDDS). The dielectric properties of bR membrane films in high-frequency range 200 kHz – 3 GHz were determined by “Dipole TDS” time-domain dielectric spectrometer (TDS-2). This spectrometer determines the dielectric properties of materials by measuring the response of a sample to an applied short rise time step of electric field. General principles of TDS and a detailed description of the setup and measurement routine has been described elsewhere.⁹ The data treatment was performed directly in the time domain in terms of the macroscopic dipole correlation functions (DCF) $\Gamma(t)$:

$$\psi(t) \approx \Gamma(t) = \frac{\langle \bar{M}(0) \cdot \bar{M}(t) \rangle}{\langle \bar{M}(0) \cdot \bar{M}(0) \rangle} \quad (1)$$

where $M(t)$ is the macroscopic fluctuation dipole moment of the sample volume unit, which is equal to the vector sum of all of the molecular dipoles, and the symbol $\langle \rangle$ denotes averaging of the ensemble. The velocity and the laws governing the decay function $\Gamma(t)$ are directly related to the structural and kinetic properties of the sample and characterize the macroscopic properties of the system under investigation.

The time domain response of the sample was determined from the accumulation of 25 600 individual scans. Nonuniform sampling of the time window (4.4 μ s) of each pulse enables the generation of spectra in the frequency range from 200 kHz up to 3 GHz. The measurement accuracy of the dielectric permittivity and losses was better than 5%.^{9–11} The accuracy of fitting (mean square deviation) was less than 10^{-3} .

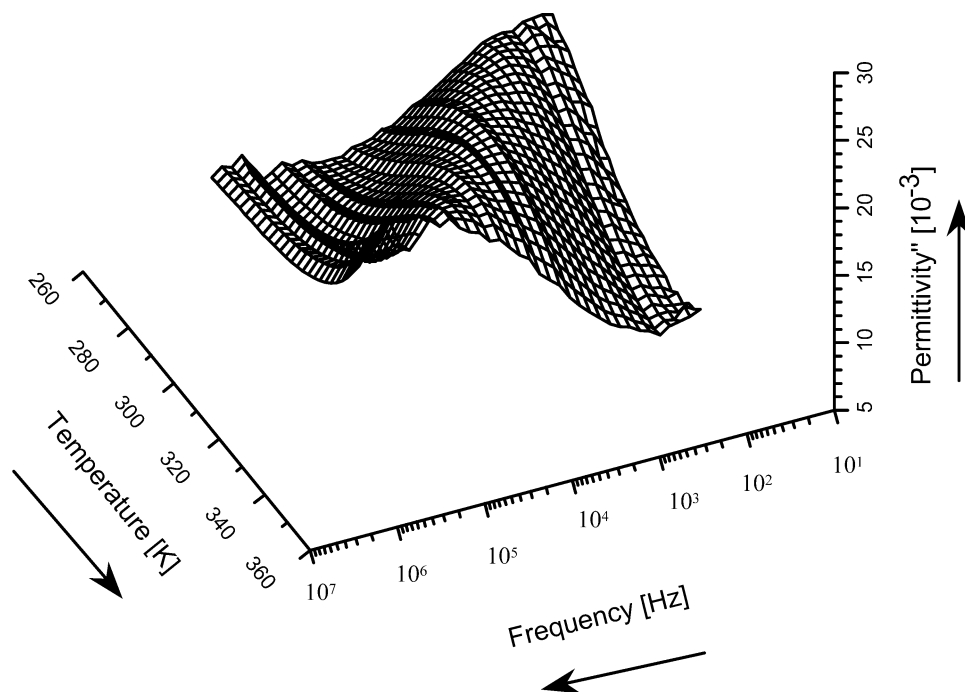
Thus, by using both spectrometers, TDS and BDS, we could overlap wide frequency range from 10 mHz up to 3 GHz.

2.3. Protocol of Experiments. In DS experiments, the temperature was varied between 5 and 70 °C. For the investigation of dielectric parameters reversibility, the special protocol, consisting of three temperature intervals, was used. Starting from room temperature, we did some temperature circles, i.e., the sample was cooled from 25 up to 5 °C (first cooling interval), then the sample was heated to 70 °C (heating interval), and afterward the sample was cooled again up to 5 °C (second cooling). The measurements have been done in all three of the temperature intervals for both oriented and nonoriented bR membrane films.

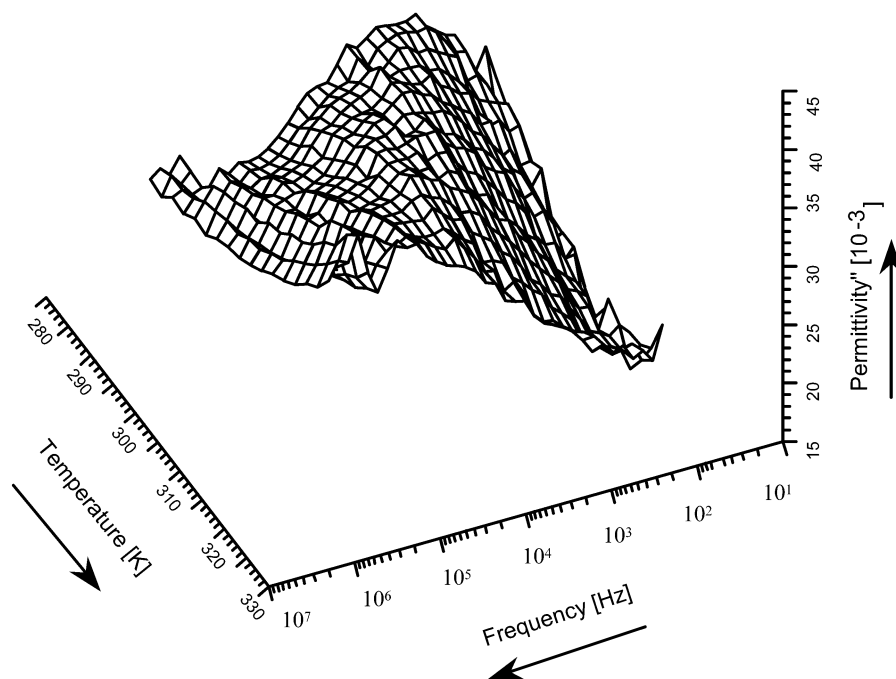
All of the measurements as a function of temperature were done at the room atmosphere at the humidity around 60%.

3. Results

3.1. Low-Frequency Measurements (BDS). The typical 3D losses spectra of the bR membrane film obtained by low-frequency BDS in the frequency range 10^{-2} up to 10^6 Hz and in the second cooling temperature interval (70–5 °C) is presented in Figure 2. The main relaxation process and partly two other processes at low and high frequencies are observed in the covered temperature and frequency intervals. For a



a. oriented membrane film



b. non-oriented membrane film

Figure 2. 3D dielectric losses spectra of the oriented (a) and nonoriented bR membrane film measured by BDS.

quantitative analysis of the dielectric behavior for the low and high-frequency parts of the spectra $\epsilon^*(\omega)$, a formula of superposition of Havriliak–Negami¹² (HN) $\Delta\epsilon/[1 + (i\omega\tau)^\alpha]^\beta + \epsilon_\infty$ and Jonscher's empirical terms¹³ for low $(i\omega)^m$ and high $(i\omega)^{(n-1)}$ frequency parts of the spectra were used. Here $\Delta\epsilon$ is the dielectric strength, τ is the mean relaxation time, and ω is

the cyclic frequency. The parameters α and β , ranging between 0 and 1, are related to the inhomogeneous characteristics of the bR membrane films; m and n are Jonscher parameters. Below we will discuss the main relaxation process, described by the Havriliak–Negami formula. We will call this dielectric response as the low-frequency dispersion (1st relaxation process).

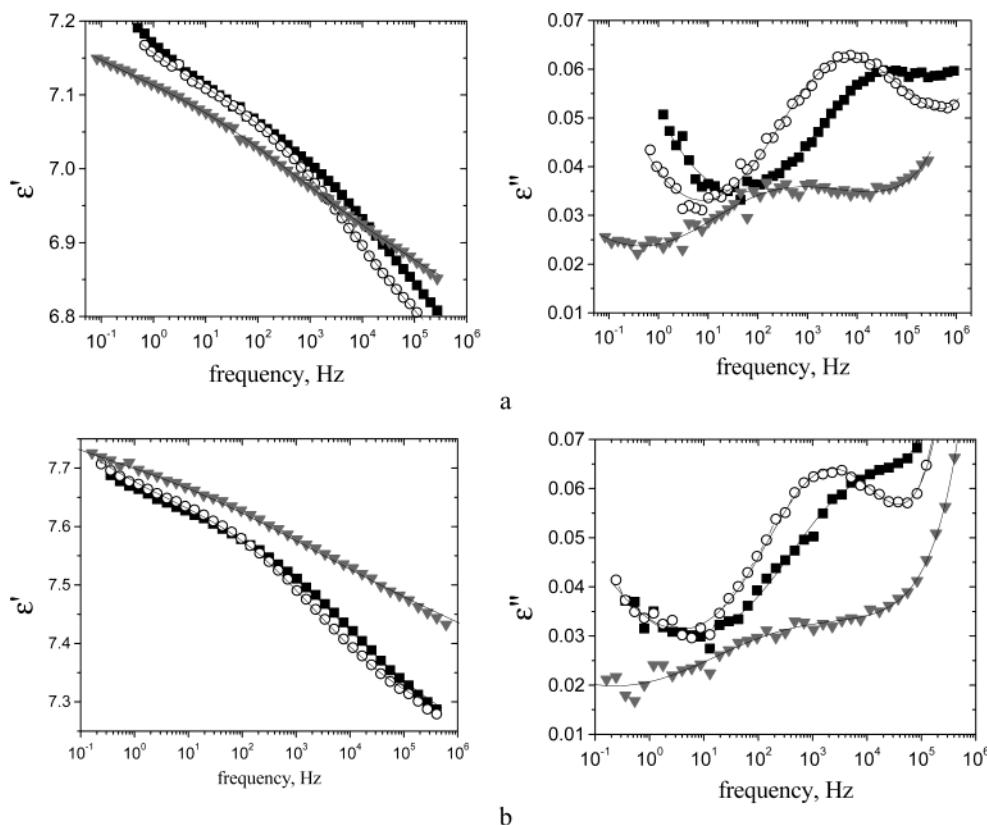


Figure 3. Spectra of the dielectric permittivity and losses at 20 °C of the nonoriented (a) and oriented (b) bR membrane films measured during first cooling (■), heating (○), and second cooling (▼).

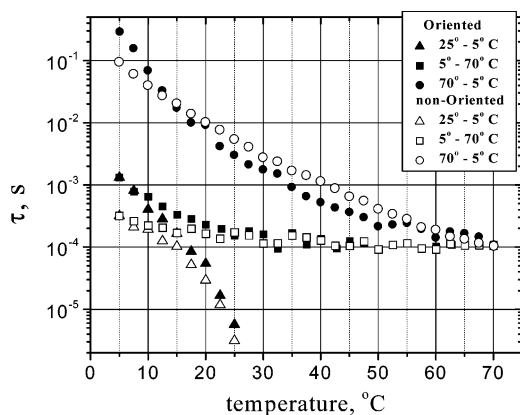


Figure 4. Relaxation time of the low-frequency process, measured by BDS for nonoriented (open signs) and oriented (solid signs) membranes. The measurements were performed in accordance with the special protocol (see Figure 3). Triangles used for first cooling, squares used for heating, and circles used for second cooling.

Three spectra at 20 °C during 1st cooling, heating, and 2nd cooling for nonoriented (Figure 3a) and oriented (Figure 3b) membrane films are presented. A significant difference between these three spectra is clearly observed. The temperature transitions in the bR membrane are not reversible and lead to some alterations in the structure of films. The nonreversible behavior of the low-frequency relaxation process ($\Delta\epsilon$ and τ) is observed also for both oriented and nonoriented membranes (see Figures 4 and 5). The maximal difference in the dielectric behavior of oriented and nonoriented membranes takes place at low temperatures.

3.2. High-Frequency Measurements (TDDS Data). The high-frequency measurements were performed in the time domain, and the macroscopic correlation functions for both types

of samples were obtained by using the temperature protocol described above. The typical example of correlation function is presented in Figure 6. One can see that the dipole correlation function has a complex nonexponential behavior. The analysis showed that the best fitting can be performed by the sum of N Debye relaxation processes as

$$F(t) = \sum_i A_i \exp(-t/\tau_i) \quad (2)$$

where τ_i are the relaxation times and A_i are the amplitudes of the processes ($\sum_{i=1}^N A_i = 1$). It was shown for bR membrane films, $N = 3$, and taking into account the low-frequency process, measured by BDS, the whole dielectric response can be described by four relaxation processes. For the nonoriented bR membrane film, the relaxation time and dielectric strength for the second, third, and fourth processes are plotted in Figure 7. The same parameters for oriented bR membrane film are presented in Figure 8. The full dielectric strength, measured by TDS, is plotted in Figure 9.

Finally, the experimental results obtained by TDS and BDS have shown that in the frequency range from 10 mHz up to 3 GHz the four relaxation processes were observed. An example of the merge dielectric spectrum evaluated by both methods at 5 °C at the first cooling is presented in Figure 10.

4. Discussion

4.1. Nature of the Relaxation Processes. Analysis of the experimental results reveals dielectric response at different time scales varying from nanoseconds up to milliseconds (see Figures 2, 6, and 10). The dielectric strengths of the processes that have very small amplitude can be explained by very modest contribution to the polarization of the restricted mobility of the permanent and induced electric dipoles in bR membrane films.

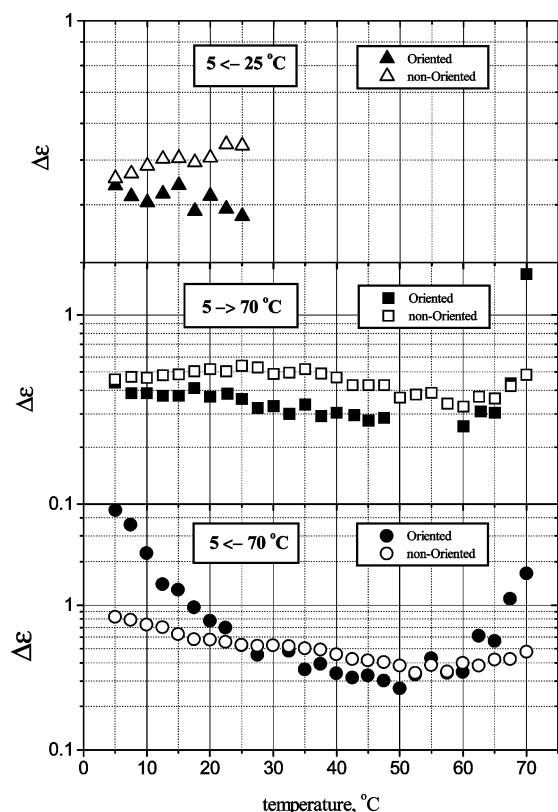


Figure 5. Dielectric strength of the low-frequency process measured by BDS for nonoriented (open signs) and oriented (solid signs) membranes. The measurements were performed in accordance with the special protocol (see Figure 3). Triangles used for first cooling, squares used for heating, and circles used for second cooling.

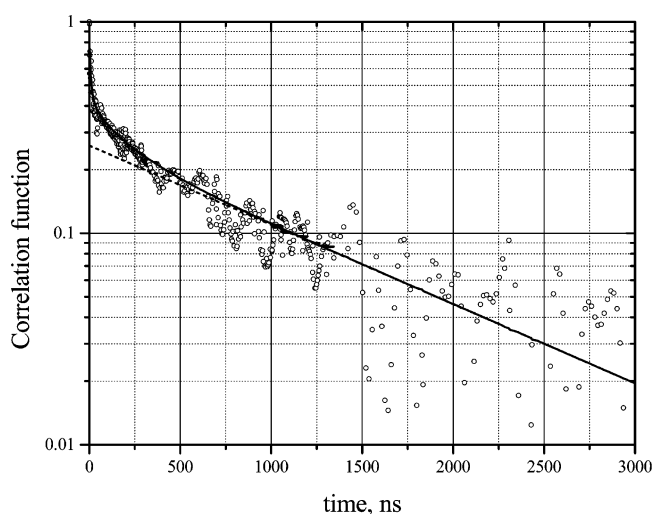


Figure 6. Dipole correlation function $\Gamma(t)$ of oriented bR membrane film at 23 °C, provided by TDDS. (O) is experimental data; the solid line corresponds to a fit by the sum of Debye relaxation processes, the dashed line shows the low-frequency process with the effective amplitude being equal to 0.26 and the correlation time being equal to 1158 ns.

It leads also to the weak signal in the TDS experiments and rather big error in determination of the dielectric strength.

Comparison of spectra at the same temperature 20 °C during 1st cooling, heating, and 2nd cooling (see Figure 3) has revealed the differences in their behavior, especially after heating. Fitting parameters of spectra in Figure 3 are presented in Table 1. Generally, the bR membrane film demonstrates nonreversible

TABLE 1: Parameters of Spectra of BR Films at 20 °C Presented in Figure 3 and Evaluated as a Result of Fitting to Havriliak–Negami Equation and Jonscher’s Empirical Terms

protocol	n	m	τ , Hz	$\Delta\epsilon$	ϵ_∞	a	b
Nonoriented Membrane Film							
1st cooling	0.788	0.812	2.92×10^{-5}	0.506	6.53	0.405	0.362
heating	0.739	0.795	1.63×10^{-4}	0.518	6.57	0.418	0.384
2nd cooling	0.828	0.715	1.02×10^{-2}	0.578	6.5	0.428	0.117
Oriented Membrane Film							
1st cooling	0.799	0.8645	5.41×10^{-5}	0.417	7.17	0.398	0.584
heating	0.806	0.871	2.29×10^{-4}	0.37	7.22	0.486	0.514
2nd cooling	0.862	0.7673	9.27×10^{-3}	0.781	6.88	0.379	0.083

TABLE 2: Structural and Dynamic Parameters of the bR Membrane Film Components: Molecular Weight (MW) or Size (d Is the Diameter; h Is the Thickness), Relaxation Time (τ), and Dipole Moment (μ)

structure units	MW or size	relaxation time, τ	dipole moment, μ [D]
full sample	$d = 10$ nm; $h = 0.03$ nm		
bR membrane fragment	$d = 5$ nm; $h = 5 \mu\text{m}^a$	100 ms ^b	$\sim 2.5 \times 10^6$ ^a
triad	~ 75 kD		~ 180 – 300
bR molecule	~ 25 kD	$\sim 1.5 \mu\text{s}^c$	60 ; ^d 98^e
α -helix	~ 3 kD		~ 60
retinal	~ 300	260 μs^b	~ 10
Am. Ac. residues	75–175	100 ps–5 ns ^f	15–35 ^f
head/lipid	$\sim 150/800$	~ 5 ns ^g	~ 12

^a Keszthelyi, 1980.⁸ Measurements were done in solution of bR membrane fragments. ^b Shinar et al., 1977.¹⁹ Measurements were done in solution of bR membrane fragments. ^c Cherry et al., 1977.¹⁵ Measurements were done in bR-incorporated liposome suspension. ^d Barabas et al., 1983.⁴ ^e Kimura et al., 1984.⁵ ^f Grant et al., 1978.²⁰ ^g Ermolina et al., 2000.²¹ Measurements were done in liposome suspension.

behavior against the temperature for changes in the low frequency dielectric response. The nonreversible temperature transitions in the bR membrane are observed most probably due to some alterations in structure of films.

To provide for a framework for the discussion of the four relaxation processes that have been detected let us consider the structural components in the bR system. Table 2 presents the structural units of the bR film and their molecular weight (or size), relaxation time, and dipole moment. The molecular weights were estimated by using the protein data bank. The dipole moment of the α helix, μ , was calculated by the simple approximation:¹⁴ $\mu = L \cdot e/2$, where L is the length of the α helix and e is the unit charge. Note that the main contribution in the dipole moment of the bR molecule gives the dipole moment of the α helices. Because six α helices among seven are compensated by each other (see Figure 1a), the dipole moment of the protein can be approximated as the dipole moment of single α helix. Really, our estimation gave ~ 60 D, which is in a good agreement with the experimental results of 60–98 D (see Table 2). The dipole moment of the triad is equal to three times the dipole moment of a single molecule because all of the bR molecules face to one side in the membrane fragment. Note the average relaxation time of the membrane fragments was measured in suspensions, whereas the relaxation time for the bR molecule was recalculated from the diffusion coefficient obtained for bR macromolecules incorporated into the phospholipid bilayer.¹⁵

Analysis of structural and dynamical parameters, with the assumption that the bigger the structure, the bigger the relaxation

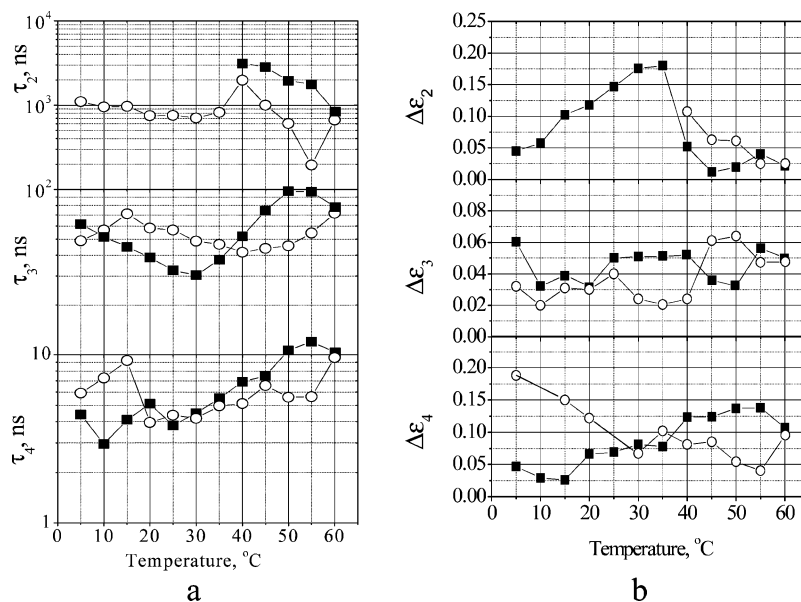


Figure 7. Relaxation times and dielectric strengths of the second (τ_2), third (τ_3), and fourth (τ_4) processes, measured by TDS for the nonoriented bR membrane film. Solid signs denote heating regime from 5 up to 70 °C; open signs denote the second cooling regime from 70 up to 5 °C.

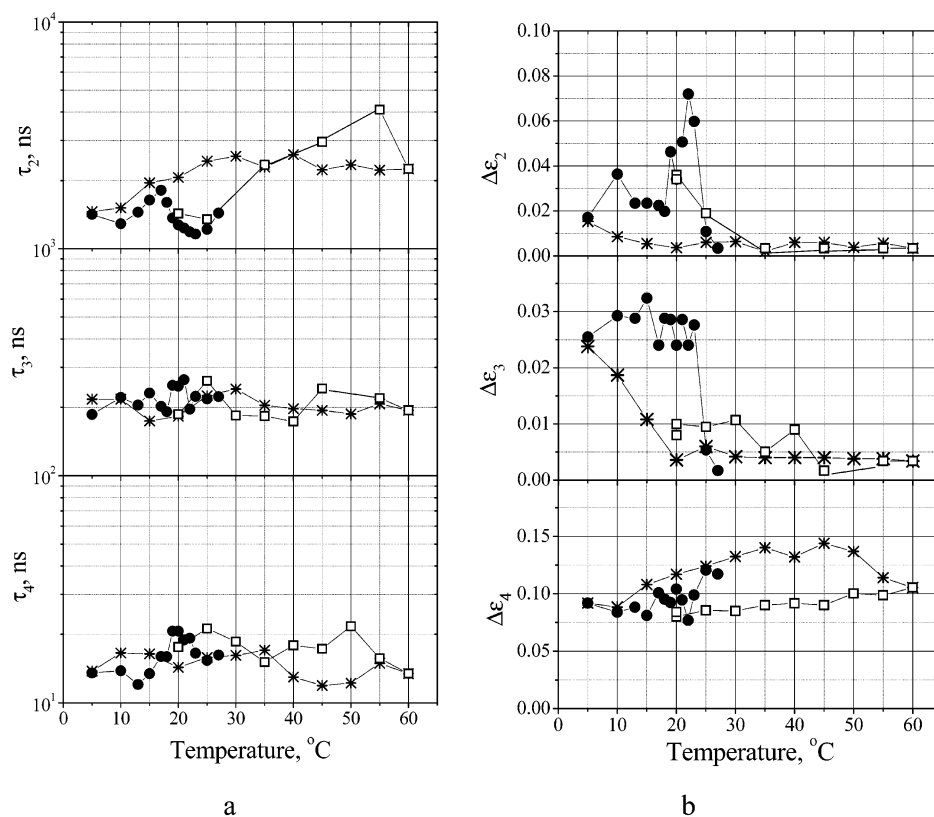


Figure 8. Relaxation times and dielectric strengths of the second (τ_2), third (τ_3), and fourth (τ_4) processes, measured by TDS for the oriented bR membrane film. (●) denotes first cooling regime from 25 up to 5 °C; (*) denotes heating regime from 5 up to 70 °C; (□) denotes second cooling from 70 up to 20 °C.

time, allows us to suggest the following mechanisms for relaxation processes in DS experiment. The second relaxation process with the characteristic time around 1 μ s can be ascribed to the anisotropic rotation of the bR molecule as a whole, because this value is close to the relaxation time ($\sim 1.5 \mu$ s) of the bR molecule in liposomes (See Table 2). The slowest process we assume to be related to the collective mobility of protein molecules at large geometric scales (like pieces of membrane or aggregates of such membrane fragments) and inter-triad organization mobility. A third relaxation process most probably

reflects the anisotropic vibration of the α helices in the membrane. The fastest process can be connected with the retinal anisotropic motion and mobility of protein polar groups and lipid headgroups.

4.2. Temperature Behavior of Dielectric Relaxation in the bR Membrane Film. The largest variations that have been seen in the temperature dependence during cooling, heating, and cooling occur in the slowest processes that we have detected in our measurements. These processes as noted above probably correspond to the behavior of associated membrane fragments

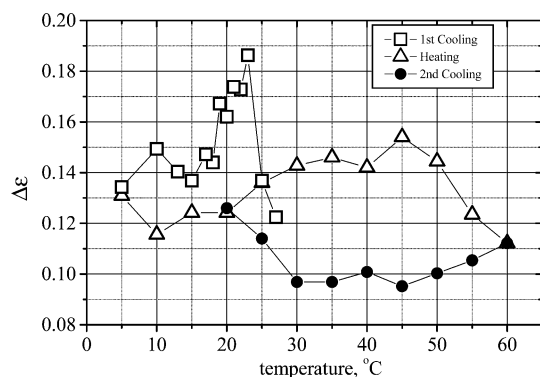


Figure 9. Temperature dependence of the dielectric strength of the oriented bR membrane film obtained in TDDS measurements. The measurements started from room temperature and continued in according with the special temperature protocol (see Figure 3). (□) denotes first cooling; (Δ) denotes heating; (●) denotes second cooling of sample. The measurement accuracy of the dielectric permittivity was better than 5%.

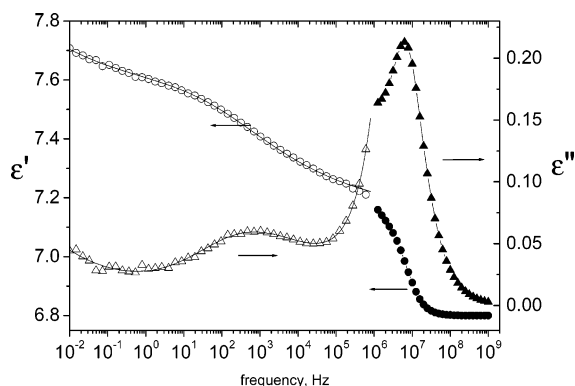


Figure 10. Merge spectrum of permittivity evaluated by both BDS (open symbols) and TDS (solid symbols) methods for oriented bR membrane at 5 °C at the first cooling.

and these large associated entities would be expected to have the slowest behavior and the largest effect of cooling, heating, and cooling. The question is how this alteration in the dielectric behavior of associated membrane fragments is correlated with the faster time response regime of the observed dielectric phenomena. In fact, in the slow processes, we see a large difference in the amplitude and in the time scale when the temperature is at the extremes in terms of cooling and heating. However, in the intermediate temperature regimes for these slow processes, the differences are less pronounced.

It is not intuitively obvious from the data that there is a direct correlation in the temperature altered dielectric phenomena of the slow and fast processes. What can be noticed, however, is that the nonoriented membrane is in general less restricted in all time scales and the amplitude of each of the processes associated with the nonoriented membranes is higher for all of the fast time scales that have been measured. In fact, if there was no connection in these fast relaxations and the slow processes, correlated with the association of membrane fragments, then it is not clear why the nonoriented and oriented membranes would exhibit any differences. This argument is based on the fact that one would expect no differences in the oriented versus the nonoriented if all of the alterations were intrafragment based. Thus, the differences in these fast time scales between oriented and nonoriented suggest that there is some contribution of membrane association to the intramembrane dielectric phenomena that we have measured.

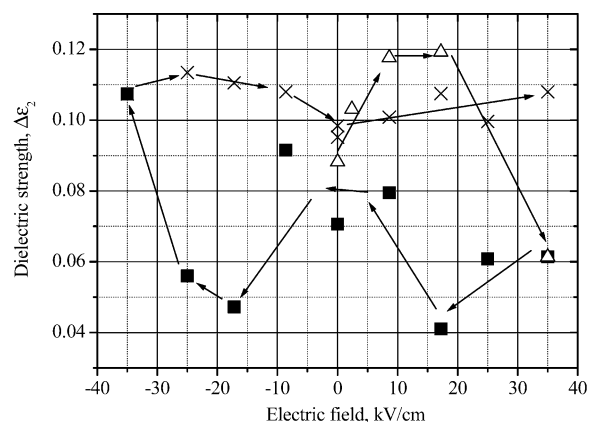


Figure 11. dc-bias field dependence of the dielectric strength at 25 °C for oriented bR membrane. The external field changed according to the following route (see arrows): from 0 to +35 Kv/cm (Δ); from +35 to -35 Kv/cm (■); from -35 to +35 Kv/cm (×). The accuracy of the dielectric strength evaluation was better than 15%.

The fastest phenomena that have been monitored are probably due to lipid motion, and here we see classic hysteresis, and this agrees with the well-known behavior of lipids in other systems. As noted below, another interesting well-marked temperature hysteresis is the low-temperature intermediate time scale behavior of the membranes (see Figure 9). This is considered in details below.

4.3. Ferroelectric Like Behavior of the Oriented bR Membrane Film. The un-expectable dielectric response for oriented bR membrane film in the low-temperature interval (5–30 °C) was revealed for all of the relaxation processes discussed in previous sections. It was observed that the most noticeable effect was recorded for the second relaxation process with the characteristic time near 1 μs (see first cooling at Figure 9). The dielectric strength demonstrates a pick near 23 °C. It appears in all our experiments on oriented bR membrane films with some shifting of the peak position and its amplitude depending on the temperature protocol. The static dielectric permittivity for the intermediate time scale process of the oriented bR membrane film shows the nonreversible behavior with the crossing the curves at 18 °C and maximal value at 23 °C. If the high-temperature loop can be explained by the well-known lipid phase transition, the low-temperature hysteresis observed in the oriented bR membrane films required a special explanation.

To understand the nature of such phenomena, the special measurements of the bR membrane by DSC and TDS at the presence an external electric field were performed. In DSC measurements, the endothermic process near 18 °C was observed for oriented membrane only.¹⁶ The TDS experiments with application of an external electric field exhibit a strong dependence of dielectric strength both on the amplitude and the direction of the field (Figure 11). For the oriented membrane film, the hysteresis behavior was determined, whereas for the nonoriented one, this effect is much smaller. Thus, these results show the presence of some transition stimulated both by temperature and an external electric field.

Note that each bR molecule has a significant dipole moment (50–100D),⁵ which has three levels of structural organization in bR membrane: macromolecular assembly of the bR molecules in the purple membrane as triads;¹⁷ the planar hexagonal structure of the protein triads¹⁷ in this membrane; and finally, planar ordering of membrane proteins as an interacting, oriented multilayered structure of membrane fragments. This specific three level structure with a dominant dipole moment oriented

in the bR protein seems to have unique ferroelectric liquid crystal properties. We have three evidences for such conclusion typical for ferroelectric behavior of some materials. First is the dc-bias hysteresis of the dielectric strength (see Figure 11). Second is the DSC peak near smectic-A–smectic-C phase transition.¹⁶ Third is the validity of the Curie–Weiss law.¹⁶ The last one was obtained by analysis of the reciprocal dielectric strength and relaxation frequency of second relaxation process vs temperature. These dependences agree with a calculation performed for a soft mode relaxation processes in ferro-electric liquid crystals near smectic-A–smectic C* ferroelectric phase transition.¹⁸

Note that this specific phenomenon is observed only for the oriented film. It could be most probably explained by the unique preparation of the oriented bR membrane film. Because the bR molecule is very stable protein, the reason for the thermal transition could be ascribed to lipid bilayer freezing and to the inter-protein interactions between the neighbor layers in the oriented membrane film. Negatively charged C terminal and positively charged N terminals of the bR molecule can interact and form a specific correlation net through the whole sample. Thus, the conformational alterations in the lipid chains permit the anisotropic motion of protein molecules in a cooperative fashion because of the protein–protein interactions.

5. Conclusions

The study of the dielectric properties of bR membrane films has shown four relaxation processes that seem to reflect the different levels of the structural organization of this complex system. Moreover, the bR membrane, prepared like oriented and nonoriented films, demonstrate different temperature dependencies. The oriented membrane films have shown a unique liquid crystal-like ferroelectric behavior. The dielectric behavior can be considered as soft mode relaxation processes in ferro-electric liquid crystals near smectic-C*–smectic-A phase transition.

Acknowledgment. We thank to Alina Strinkovski for the preparation of bR membrane films. The authors also wish to

express their gratefulness to Professor F. Kremer for allowing part of the measurements to be carried out in his laboratory and Mrs. Anna Gutina for providing the BDS experiments.

References and Notes

- (1) Shen, Yi.; Safinya, C. R.; Liang, K. S.; Ruppert, A. F.; Rothschild, K. *J. Nature* **1993**, *366*, 48–50.
- (2) (a) Birge, R. *Annu. Rev. Phys. Chem.* **1990**, *41*, 683–733. (b) Lewis, A. *Proc. Natl. Acad. Sci. U.S.A.* **1978**, *75*, 543–547. (c) Xu, D.; Martin, C.; Schulten, K. *Biophys. J.* **1996**, *70*, 453–460.
- (3) Ottolenghi, M.; Sheves, M. *Isr. J. Chem.* **1995**, *35*, 193–513.
- (4) Barabas, K.; Der, A.; Dancshazy, Zs.; Ormos, P.; Keszthelyi, L.; Marden, M. *Biophys. J.* **1983**, *43*, 5–11.
- (5) Kimura, Y.; Fujiwara, M.; Ikegami, A. *Biophys. J.* **1984**, *45*, 615–625.
- (6) Heyn, M. P.; Cherry, R. J.; Muller, U. *J. Mol. Biol.* **1977**, *117*, 607–620.
- (7) Varo, G. *Acta Biol. Acad. Sci. Hung.* **1982**, *32*, 301–310.
- (8) Keszthelyi, L. *Biochem. Biophys. Acta* **1980**, *598*, 429–436.
- (9) Feldman, Yu.; Andrianov, A.; Polygalov, E.; Ermolina, I.; Romanychev, G.; Zuev, Y.; Milgotin, B. *Rev. Sci. Instrum.* **1996**, *67*, 3208–3216.
- (10) Ermolina, I. V.; Polygalov, E. A.; Romanychev, G. D.; Zuev, Yu. F.; Feldman, Yu. D. *Rev. Sci. Instrum.* **1991**, *62*, 2262–2265.
- (11) Romanychev, G. D.; Ermolina, I. V.; Polygalov, E. A.; Zuev, Yu. F.; Ubshincki, D. V.; Feldman, Yu. D. *Russ. J. Meas. Tech.* **1992**, *35*, 61–63.
- (12) Böttcher, C. J. F.; Bordewijk, P. *Theory of Electric Polarization*, 2nd ed.; Elsevier Science B.V.: Amsterdam, 1992; Vol. 2.
- (13) Böttcher, C. J. F. *Theory of Electric Polarization*, 2nd ed.; Elsevier Science B.V.: Amsterdam, 1992; Vol. 1.
- (14) Pethig, R. *IEEE Trans. Elect. Insul.* **1984**, *EI-19*, 453–474.
- (15) Cherry, R. J.; Muller, U.; Schneider, G. *FEBS Lett.* **1977**, *80*, 465–469.
- (16) Ermolina, I.; Lewis, A.; Feldman, Yu. *J. Phys. Chem. B* **2001**, *105*, 2673–2676.
- (17) Shen, Yi.; Safinya, C. R.; Liang, K. S.; Ruppert, A. F.; Rothschild, K. *J. Nature* **1993**, *366*, 48–50.
- (18) Carlsson, T.; Zeks, B.; Filipic, C.; Levstik, A. *Phys. Rev. A* **1990**, *42*, 877–889.
- (19) Shinar, R.; Druckmann, S.; Ottolenghi, M.; Korenstein, R. *Biophys. J.* **1977**, *19*, 1–5.
- (20) Grant, E. H.; Sheppard, R. J.; South, G. P. *Dielectric behaviour of molecules in solution*; Clarendon Press: Oxford, 1978.
- (21) Ermolina, I.; Smith, G.; Ryabov, Ya.; Puzenko, A.; Polevaya, Yu.; Nigmatullin, R.; Feldman, Yu. *J. Phys. Chem. B* **2000**, *104*, 1373–1381.